Article
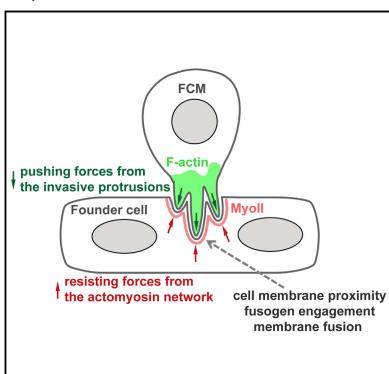
Mechanical Tension Drives Cell Membrane Fusion

Graphical Abstract

Authors

Ji Hoon Kim, Yixin Ren, ...,
Douglas N. Robinson,
Elizabeth H. Chen

Correspondence

echen@jhmi.edu

In Brief

Cell-cell fusion is induced by invasive protrusions from an "attacking" cell. Kim et al. show that the "receiving" cell mounts a mechanosensory response. The protrusive and resisting forces from two fusion partners put the fusogenic synapse under high mechanical tension, which helps to overcome energy barriers for membrane apposition and drives cell membrane fusion.

Highlights

- Invasive protrusions trigger a mechanosensory response in a cell-fusion partner

- Mechanosensory function of MyoII directs its accumulation at the fusogenic synapse

- MyoII increases cortical tension and promotes fusion pore formation

- Mechanical tension at the fusogenic synapse drives cell membrane fusion

CellPress

Mechanical Tension Drives Cell Membrane Fusion

Ji Hoon Kim,[1] Yixin Ren,[2] Win Pin Ng,[3] Shuo Li,[1] Sungmin Son,[3] Yee-Seir Kee,[2] Shiliang Zhang,[1] Guofeng Zhang,[4] Daniel A. Fletcher,[3] Douglas N. Robinson,[2] and Elizabeth H. Chen[1,*]

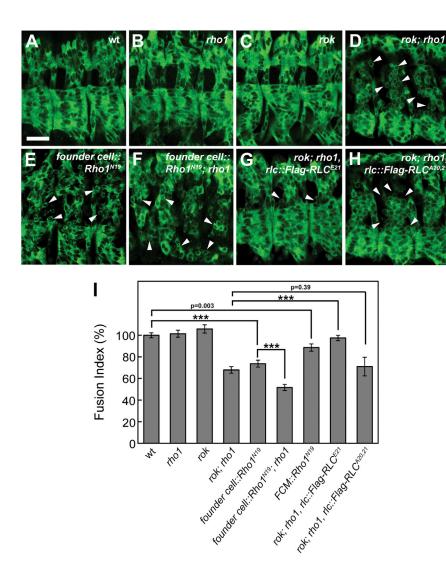[1]Department of Molecular Biology and Genetics
[2]Department of Cell Biology
Johns Hopkins University School of Medicine, Baltimore, MD 21205, USA
[3]Department of Bioengineering, University of California, Berkeley, Berkeley, CA 94720, USA
[4]Laboratory of Bioengineering and Physical Science, National Institute of Biomedical Imaging and Bioengineering, NIH, Bethesda, MD 20892, USA
*Correspondence: echen@jhmi.edu
http://dx.doi.org/10.1016/j.devcel.2015.01.005

SUMMARY

Membrane fusion is an energy-consuming process that requires tight juxtaposition of two lipid bilayers. Little is known about how cells overcome energy barriers to bring their membranes together for fusion. Previously, we have shown that cell-cell fusion is an asymmetric process in which an "attacking" cell drills finger-like protrusions into the "receiving" cell to promote cell fusion. Here, we show that the receiving cell mounts a Myosin II (MyoII)-mediated mechanosensory response to its invasive fusion partner. MyoII acts as a mechanosensor, which directs its force-induced recruitment to the fusion site, and the mechanosensory response of MyoII is amplified by chemical signaling initiated by cell adhesion molecules. The accumulated MyoII, in turn, increases cortical tension and promotes fusion pore formation. We propose that the protrusive and resisting forces from fusion partners put the fusogenic synapse under high mechanical tension, which helps to overcome energy barriers for membrane apposition and drives cell membrane fusion.

INTRODUCTION

Membrane fusion occurs in a diverse array of biological processes, including viral entry (Kielian and Rey, 2006; Melikyan, 2008), intracellular trafficking (Doherty and McMahon, 2009; Jahn and Fasshauer, 2012), and fusion between cells (Aguilar et al., 2013; Chen and Olson, 2005; Sapir et al., 2008). It is an energy-consuming process in which two initially separate lipid bilayers merge into one. For membrane fusion to occur, several energy barriers have to be overcome. These include bringing together two membranes containing repulsive charges and the subsequent destabilization of the apposing lipid bilayers, leading to fusion pore formation and expansion. Studies of intracellular vesicle fusion have led to the identification of many proteins, including SNAREs, SM proteins, synaptotagmins, and Rabs, which are required for tight juxtaposition of vesicle and target membranes (Jahn and Fasshauer, 2012; Jahn and Südhof,

1999; Martens and McMahon, 2008). However, relatively little is known about how cells overcome the energy barriers to fuse their plasma membranes during intercellular fusion.

Previously, we have shown in both *Drosophila* embryos and a reconstituted cell-fusion culture system that cells utilize actin-propelled membrane protrusions to promote fusogenic protein engagement and fusion pore formation (Chen, 2011; Duan et al., 2012; Jin et al., 2011; Sens et al., 2010; Shilagardi et al., 2013). In *Drosophila* embryos, the formation of multinucleate body-wall muscles requires fusion between two types of muscle cells, muscle founder cells and fusion-competent myoblasts (FCMs) (Abmayr et al., 2008; Chen and Olson, 2004; Rochlin et al., 2010). Prior to myoblast fusion, a founder cell and an FCM form an adhesive structure, which we named "fusogenic synapse" (Chen, 2011; Sens et al., 2010), mediated by two pairs of immunoglobulin (Ig)-domain-containing cell adhesion molecules, Dumbfounded (Duf) and its paralog Roughest (Rst) in the founder cell (Ruiz-Gómez et al., 2000; Strünkelnberg et al., 2001) and Sticks and stones (Sns) and its paralog Hibris in the FCM (Artero et al., 2001; Bour et al., 2000; Dworak et al., 2001; Shelton et al., 2009). These cell-type-specific adhesion molecules organize distinct actin cytoskeletal rearrangements in the two adherent muscle cells, resulting in the formation of asymmetric F-actin structures at the fusogenic synapse (Abmayr and Pavlath, 2012; Chen, 2011; Haralalka et al., 2011; Sens et al., 2010). Specifically, the "attacking" FCM generates an F-actin-enriched podosome-like structure (PLS), which invades the "receiving" founder cell; the latter forms a thin sheath of actin underlying its plasma membrane (Chen, 2011; Sens et al., 2010). In a reconstituted cell culture system, the S2R+ cells, which are of hemocyte origin and do not express muscle-cell-specific cell adhesion molecules, can be induced to fuse at high frequency by incubating cells coexpressing the FCM-specific cell adhesion molecule Sns and a *C. elegans* fusogenic protein Eff-1 with cells expressing Eff-1 only (Shilagardi et al., 2013). This cell culture system mimics the asymmetric actin cytoskeletal rearrangements during *Drosophila* myoblast fusion in that it also requires actin-propelled PLS protruding from the Sns-Eff-1-expressing attacking cells into the Eff-1-expressing receiving cells (Shilagardi et al., 2013). The invasive protrusions from the attacking fusion partners in both *Drosophila* embryo and cultured S2R+ cells appear to impose a mechanical force on the receiving fusion partners, since they cause inward curvatures on the latter (Sens et al., 2010; Shilagardi et al., 2013). However, previous

Figure 1. Founder-Cell-Specific Function of Rho1, Rok, and MyoII in *Drosophila* Myoblast Fusion

(A–H) Stage 15 embryos were labeled with α-muscle MHC antibody. Ventral lateral muscles of three hemisegments are shown in each panel. Anterior is at the left and posterior is at the right. (A) Wild-type (WT). (B and C) Normal myoblast fusion in *rho1* (B) and *rok* (C) mutant. (D) Myoblast fusion defect in *rok; rho1* double mutant. (E and F) Expressing a dominant-negative form of Rho1, Rho1^{N19}, in founder cells of WT (E) and *rho1* mutant (F) caused myoblast fusion defects. Note the more severe defect in (F) than in (E). (G and H) Expression of a phosphomimetic form of RLC, RLC^{E21} (G), but not a nonphosphorylatable form, RLC^{A20,21} (H), rescued the fusion defect in *rok; rho1* double mutant. Arrowheads indicate unfused FCMs. Bar, 20 μm.

(I) Quantification of myoblast fusion. The fusion index was determined as the percentage of the number of Ladybird early-positive nuclei in mutant versus WT segmental border muscles (SBMs). Error bars indicate SEM. ***$p < 10^{-4}$.

See also Figure S1 and Table S1.

studies have not revealed how these invasive protrusions affect the mechanics of the receiving cells.

Cellular response to mechanical force is critical for diverse biological processes such as tissue morphogenesis, growth control, and cell fate specification (Discher et al., 2009; Farge, 2011; Gauthier et al., 2012; Guillot and Lecuit, 2013; Mammoto et al., 2013; Vogel and Sheetz, 2009). The nonmuscle Myosin II (MyoII) is a well-known intracellular effector of mechanosensory responses (Aguilar-Cuenca et al., 2014; Gauthier et al., 2012; Guillot and Lecuit, 2013; Lecuit et al., 2011; Mammoto et al., 2013; Zajac and Discher, 2008). MyoII is activated by chemical signaling pathways, one of which involves cell surface proteins such as integrin, the Rho GTPase, and Rho kinase (Rok) (Amano et al., 1996). Activated MyoII, in turn, generates contractile force to regulate cellular behaviors such as migration, adhesion, and shape change. However, what initiates MyoII recruitment to cellular locations in response to mechanical stimuli remains unclear. A prevailing model based on genetic analysis in many cell types suggests that MyoII is recruited by chemical signaling, involving integrin, Rho, and Rok. Alternatively, recent biophysical studies demonstrated that MyoII can be repositioned by externally applied mechanical force (Effler et al., 2006; Fernandez-Gonzalez et al., 2009; Luo et al., 2013; Ren et al., 2009), and this effect is through MyoII's direct sensing of mechanical tension (Luo et al., 2013; Ren et al., 2009).

In this study, we demonstrate that, during cell-cell fusion, the receiving fusion partner mounts a MyoII-mediated mechanosensory response to the invasive force from the attacking cell at the fusogenic synapse. MyoII is recruited to the fusogenic synapse because of its intrinsic ability to sense mechanical strains in the actin network, whereas chemical signaling from cell adhesion molecules, Rho, and Rok increases the amount of activated MyoII and amplifies the mechanosensory response of MyoII. The accumulated MyoII generates additional cortical tension required for resisting the PLS invasion, thereby promoting cell membrane juxtaposition and fusion.

RESULTS

Rho1, Rok, and MyoII Promote *Drosophila* Myoblast Fusion

In a genetic screen for new components involved in *Drosophila* myoblast fusion, we identified a function for Rho1, Rok, and MyoII. Although zygotic single mutants of these genes did not exhibit a myoblast fusion defect due to maternal contribution (Figures 1A–1C and 1I; Figures S1C and S1L; Table S1), mutations in *rho1* and *myoII* significantly enhanced the fusion defect caused by a hypomorphic mutation in the founder-cell-specific adhesion molecule Duf, *duf*^{fp} (Figures S1D, S1E, S1G, and S1L; Table S1). In addition, *rho1* enhanced the fusion defect
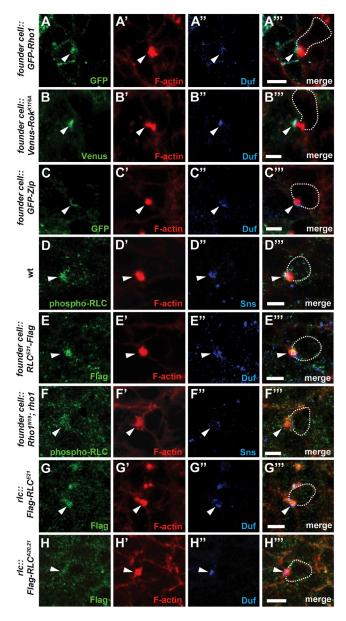
Figure 2. Localization of Rho1, Rok, and MyoII at the Fusogenic Synapse

Fusogenic synapses (arrowheads) in stage 14 embryos marked by F-actin foci (phalloidin; red) and cell adhesion molecules Duf or Sns (α-Duf or Sns; blue). The attacking FCMs are outlined in the merged panels except for the area of the fusogenic synapse, the plasma membrane within which is impossible to delineate at this resolution.

(A–C''') Founder-cell-specific accumulation of Rho1, Rok, and MyoII at the fusogenic synapse. Fluorescently tagged Rho1 (A–A'''), Rok[K116A] (a kinase-dead form; Simões et al., 2010) (B–B'''), and Zip (C–C''') were specifically expressed in founder cells and visualized by α-GFP staining (green).

(D–F''') MyoII activation at the fusogenic synapse. Activated MyoII RLC was visualized by α-phospho-RLC staining (green) (D and F) or by α-Flag staining (green) of founder cell-expressed phosphomimetic RLC[E21]-Flag (E). Note the enrichment of phospho-RLC and RLC[E21] at the fusogenic synapse in wild-type (WT) (D and E) and the markedly reduced accumulation of phospho-RLC in embryo with decreased Rho1 activity (F).

(G–H''') RLC phosphorylation is required for its accumulation at the fusogenic synapse. Flag-tagged RLC[E21], or nonphosphorylatable RLC, RLC[A20, 21], was expressed with the endogenous *rlc* promoter and visualized by α-Flag staining

caused by the loss of *elmo*, which encodes a subunit of a Rac GEF (Geisbrecht et al., 2008) (Figures S1H, S1I, and S1L; Table S1), and the *rok; rho1* double mutant also exhibited a fusion-defective phenotype (Figures 1D and 1I; Table S1). It is interesting that founder-cell-specific expression of a dominant-negative form of Rho1 (Rho1[N19]) disrupted fusion in wild-type embryos and, more significantly, in *rho1* mutant embryos (Figures 1E, 1F, and 1I; Table S1), whereas FCM-specific expression of Rho1[N19] caused a less severe fusion defect, which could be due to the diffusion of Rho1[N19] from FCMs to founder cells after cell fusion (Figure 1I; Table S1). These data suggest that Rho1 may function in founder cells. In support of this, founder-cell-specific, but not FCM-specific, expression of Rho1 restored fusion in the *elmo; rho1* double mutant to the level of the *elmo* single mutant, demonstrating a specific function of Rho1 in founder cells (Figures S1J–S1L; Table S1). To investigate whether Rho1 and Rok function through the Rho1 → Rok → MyoII pathway, we examined the ability of phosphorylated MyoII regulatory light chain (RLC) to rescue the fusion defect in *rho1; rok* double-mutant embryos. Indeed, expression of a phosphomimetic active form of RLC, RLC[E21] (in which the Rok phosphorylation site is changed to Glu)—but not the nonphosphorylatable inactive form, RLC[A20,21]—with the endogenous *rlc* promoter rescued the fusion defect in *rok; rho1* double-mutant embryos (Figures 1G–1I; Table S1). Moreover, expression of RLC[E21] in founder cells of *duf[rp]; rho1* double-mutant embryos restored fusion to the level of the *duf[rp]* single mutant (Figures S1F and S1L; Table S1). Thus, the principal requirement of the Rho1-Rok pathway in myoblast fusion is to activate MyoII by phosphorylating its RLC in founder cells.

Rho1, Rok, and MyoII Are Enriched at the Fusogenic Synapse in Founder Cells

To investigate the subcellular localization of Rho1, Rok, and MyoII, we first performed antibody-labeling experiments using an α-Rho1 antibody to detect the endogenous Rho1 or an α-GFP antibody to detect GFP-Rho1 under the control of the endogenous *rho1* promoter. Both endogenous Rho1 and GFP-Rho1 were enriched at the fusogenic synapse and partially colocalized with the founder-cell-specific adhesion molecule Duf (Figures S2A and S2B). However, it was difficult to delineate the potential sidedness of Rho1 localization simply by confocal imaging of endogenous Rho1 or rho1::GFP-Rho1 due to the limited resolution of the confocal microscopy (200 nm), the tight juxtaposition of two adherent membranes (~10 nm thickness), and the 3D configuration of the fusogenic synapse. Indeed, partially "overlapping" signals of the founder-cell-specific Duf and the FCM-specific F-actin foci at the fusogenic synapse are frequently observed by confocal imaging (Sens et al., 2010). Therefore, we expressed GFP-Rho1 in a cell-type-specific manner to determine the potential sidedness of its accumulation. As shown in Figure 2A, GFP-Rho1 specifically expressed in founder cells accumulated at the fusogenic synapse. To assess the localization of GFP-Rho1 in FCMs, we took advantage of a fusion

(G and H). Note the high level accumulation of RLC[E21] (G), but not RLC[A20,21] (H), at the fusogenic synapse. Bars, 5 μm.
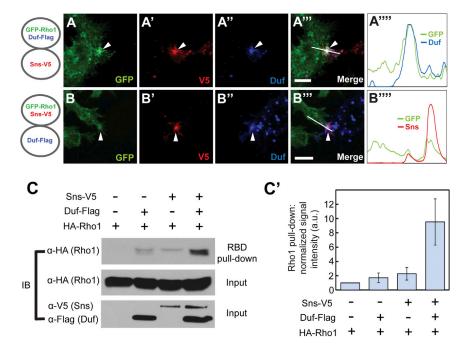See also Figures S2 and S3.

Figure 3. Rho1 Is Recruited and Activated by Duf upon Sns Binding

(A–A''') S2R+ cells coexpressing GFP-Rho1 (green) and Duf-Flag (blue) were mixed with cells expressing Sns-V5 (red). Note the accumulation of Rho1 at the cell-cell contact site (arrowhead). (A'''') The relative intensity of Rho1 and Duf along the marked line in (A''') was plotted. Bar, 5 μm.

(B–B''') S2R+ cells coexpressing GFP-Rho1 (green) and Sns-V5 (red) were mixed with cells expressing Duf-Flag (blue). Note the lack of Rho1 enrichment at the cell-cell contact site (arrowhead). Bar, 5 μm.

(B'''') Intensity plot along the marked line in (B''').

(C and C') Increased Rho1 activity in cells coexpressing Rho1 and Duf upon Duf-Sns interaction. (C) Rho1 protein was pulled down by the RBD of Rhotekin. Note the enhanced level of Rho1 pull down when cells coexpressing Duf and Rho1 were mixed with cells expressing Sns. (C') Quantification of Rho1 pull-down levels from three independent experiments. Error bars indicate SEM.

mutant, *solitary* (*sltr*) (Kim et al., 2007), in which FCM-expressed GFP-Rho1 was retained in FCMs due to defects in myoblast fusion. As shown in Figure S2C, GFP-Rho1 expressed in FCMs did not accumulate at the fusogenic synapse. Thus, Rho1 is specifically recruited to the fusogenic synapse in founder cells. In contrast to wild-type embryos, Rho1 showed no specific enrichment in *duf, rst* double-mutant embryos (Figure S2D), in which founder cells and FCMs fail to adhere, leading to a complete fusion defect (Strünkelnberg et al., 2001), thus demonstrating that Rho1 recruitment to the fusogenic synapse is dependent on muscle cell adhesion mediated by the functionally redundant cell adhesion molecules Duf and Rst. To assess whether the Rho1 recruited by Duf and Rst is activated, we performed pull-down experiments in *Drosophila* S2R+ cells using the Rhotekin Rho-binding domain (RBD), which selectively binds to the GTP-bound active Rho1. As shown in Figure 3, Rho1 was recruited to cell-cell contact sites when it was cotransfected with Duf, but not Sns (Figures 3A and 3B), and the recruited Rho1 was activated, shown by enhanced pull down by RBD compared with controls (Figures 3C and 3C').

Like Rho1, Rok and MyoII (both myosin heavy chain [MHC], Zipper [Zip], and regulatory light chain [RLC]) showed accumulation at the fusogenic synapse (Figures S2E–S2G), and their accumulation was exclusive in founder cells (Figures 2B and 2C) but not FCMs (Figures S2H and S2I; Figure S3A). Such accumulation was not due to an increased amount of F-actin, since no obvious actin accumulation at the fusogenic synapse was observed in founder cells (Sens et al., 2010). Moreover, phosphorylated RLC was also enriched at the fusogenic synapse, visualized by either an α-phospho-RLC antibody (Figure 2D) or an α-Flag antibody against the phosphomimetic form Flag-RLC[E21] specifically expressed in founder cells (Figure 2E), demonstrating that the accumulated MyoII in founder cells is also activated. Notably, in *sltr* mutant embryos where GFP-Zip was absent in FCMs (Figure S2I), MyoII still accumulated at the fusogenic synapse

visualized by α-phospho-RLC antibody (Figure S2J), presumably due to prolonged presence of cell adhesion molecules (Kim et al., 2007) and enrichment of MyoII in founder cells (Figure 2C). MyoII activation at the fusogenic synapse required Rho1 activity, as shown by the significantly reduced level of phospho-RLC in *rho1* mutant embryos expressing Rho1[N19] in founder cells (hereinafter, these embryos are referred to as *founder cell::Rho1[N19]; rho1*) (Figure 2F). In addition, Rok activity was also critical for MyoII activation, demonstrated by the high-level accumulation of RLC[E21], but not RLC[A20,21], at the fusogenic synapse (Figures 2G and 2H).

MyoII Can Be Recruited to the Fusogenic Synapse Independently of Duf-Mediated Rho1 Signaling in *Drosophila* Embryos

Although MyoII activation requires the presence of Rho1 and Rok in the cytoplasm, it was unclear whether MyoII accumulation at the fusogenic synapse is triggered by the Duf/Rst-initiated signaling to Rho1. To address this question, we analyzed *duf, rst* double-mutant embryos expressing a truncated Duf protein that lacks its entire intracellular domain (DufΔintra). DufΔintra can attract FCMs with its intact ectodomain and mediate normal muscle cell adhesion, demonstrated by the presence of normal invasive PLSs in DufΔintra-expressing *duf, rst* mutant embryos. However, DufΔintra fails to transduce any chemical signal from plasma membrane to Rho1, as Rho1 exhibited no accumulation at the majority (80.3%, n = 56) of the muscle cell adhesion sites compared with other regions of the cell cortex (Figures 4A and 4E), whereas Rho1 showed normal accumulation at the fusogenic synapse in DufΔintra-expressing wild-type embryos (Figure S3B). Despite the absence of Rho1 recruitment, MyoII (Zip) still accumulated at the majority of these adhesion sites and colocalized with DufΔintra (Figure 4B). Specifically, while strong MyoII accumulation (≥2-fold enrichment) was observed at 82.1% (n = 56) fusogenic synapses in wild-type embryos,
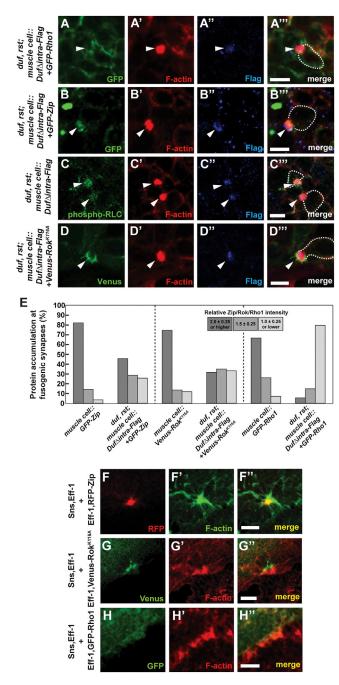
Figure 4. MyoII and Rok Enrichment at the Fusogenic Synapse Is Independent of Duf-Mediated Rho1 Signaling

(A–D‴) Fusogenic synapses (arrowheads) in stage 14 embryos marked by F-actin foci (phalloidin; red) and DufΔintra (α-Flag; blue). (A–A‴) Rho1 recruitment to the fusogenic synapse is dependent on the intracellular domain of Duf. GFP-Rho1 was expressed with DufΔintra-Flag in all muscle cells in *duf,rst* double mutant. Note the lack of Rho1 enrichment at the fusogenic synapse. (B–D‴) Accumulation of activated MyoII and Rok at the fusogenic synapse in DufΔintra-expressing *duf,rst* double-mutant embryos. Note the enrichment of GFP-Zip (B), activated RLC (α-phospho-RLC) (C), and Venus-Rok[K116A] (D) at the fusogenic synapse.

(E) The relative intensity of Zip, Rok, and Rho1 enrichment at fusogenic synapses in wild-type and DufΔintra-expressing *duf,rst* double-mutant embryos. The intensity of fluorescent signal at the fusogenic synapse was compared with that in the adjacent cortical region. Note that in DufΔintra-expressing

45.7% (n = 70) of those in DufΔintra-expressing *duf, rst* mutant embryos showed a similar level of MyoII accumulation, and 28.6% showed an intermediate level of MyoII accumulation (∼1.5-fold enrichment) (compare with 14.3% in wild-type embryos) (Figures 4B and 4E). As a control, MyoII accumulation was unaffected by DufΔintra expression in wild-type embryos (Figure S3D). Moreover, strong phospho-RLC signal was detected at 36.4% (n = 44) of muscle cell adhesion sites, confirming that the accumulated MyoII was activated (Figure 4C). Corresponding to MyoII activation, 31.7% of the muscle cell adhesion sites (n = 76) showed strong Rok accumulation (Figures 4D and 4E), and Rok accumulation was unaffected by DufΔintra expression in wild-type embryos (Figure S3C). Thus, even in the absence of Duf-induced Rho1 accumulation and activation, MyoII and Rok can still accumulate and be activated at the muscle cell adhesion sites in founder cells, albeit less robustly than wild-type (Figure 4E). The partial activation of MyoII likely accounts for the partial rescue of myoblast fusion by DufΔintra in *duf, rst* double-mutant embryos (Bulchand et al., 2010).

To investigate whether MyoII and Rok accumulation in the absence of Duf/Rst-induced Rho1 enrichment at the fusogenic synapse could be due to chemical signaling from other adhesion molecules, we examined the localization of integrin, E-cadherin, and N-cadherin at muscle cell adhesion sites in the DufΔintra-expressing *duf, rst* embryos. As shown in Figure S4, none of these adhesion molecules showed any specific enrichment at the muscle cell adhesion sites. These results, together with previous reports showing that integrins and cadherins are not required for myoblast fusion (Dottermusch-Heidel et al., 2012; Prokop et al., 1998), argue against the involvement of these adhesion molecules in the adhesion of FCMs to founder cells and chemical signaling. Instead, the accumulation of MyoII and Rok in the absence of Duf-mediated Rho1 signaling may be triggered by other types of stimuli, such as the mechanical force imposed by the FCM-specific invasive PLS at the fusogenic synapse.

Rho1-Independent MyoII Recruitment to the Fusogenic Synapse in S2R+ Cells

To further probe MyoII accumulation at the fusogenic synapse in the absence of Duf-induced Rho1 signaling, we took advantage of a reconstituted cell-fusion culture system using *Drosophila* S2R+ cells (Shilagardi et al., 2013). In this culture system, Sns-Eff-1-expressing attacking cells generate actin-propelled PLSs, which invade the Eff-1-expressing receiving cells to induce high-percentage of cell-cell fusion. Knocking down MyoII by RNAi in the receiving cells, but not in the attacking cells, led to a significant decrease in cell-cell fusion without affecting Sns or Eff-1 expression, suggesting that MyoII specifically functions in the receiving cells as in *Drosophila* embryos (Figures S5A and

---

duf,rst double-mutant embryos, >70% of fusogenic synapses showed significant (>1.5-fold) Zip and Rok enrichment, whereas <20% showed Rho1 enrichment (n > 40 for each protein).

(F–H″) MyoII and Rok, but not Rho1, accumulate at the fusogenic synapse in the receiving S2R+ cells. Attacking cells expressing Sns and Eff-1 generated F-actin-enriched foci (F′, G′, and H′). The receiving cells expressed Eff-1 and RFP-Zip (F), Venus-Rok[K116A] (G) or GFP-Rho1 (H).
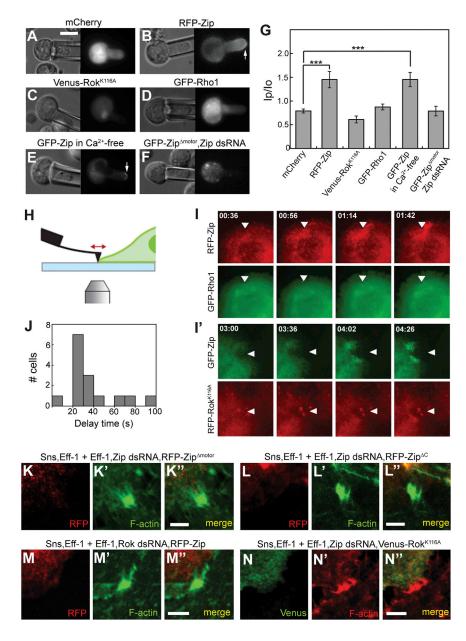
Bars, 5 µm.

See also Figure S4.

Figure 5. MyoII Functions as a Mechanosensor for Cortical Stress Independently of Rho and Rok

(A–G) MyoII accumulation in response to mechanical stress revealed by the MPA assay. (A–F) Representative differential interference contrast (DIC) (left) and fluorescent (right) images of S2 cells aspirated using micropipettes. Fluorescent proteins expressed are indicated above the panels. Note the lack of accumulation of mCherry (A), Rok[K116A] (C), Rho1 (D), and Zip[Δmotor] (F), but the accumulation of Zip (arrow) in normal (B) and Ca^{2+}-free medium (E). (G) Quantification of protein accumulation at the tip of aspirated cells. Background-subtracted protein pixel intensities at the tip of the cell body within the pipette (Ip) and at the opposite pole of the cell body (Io) were measured, and the ratio (Ip/Io) was calculated and used for statistical analysis. ***p < 10^{−4}. Error bars indicate SEM.

(H–J) MyoII accumulation in response to mechanical stress revealed by AFM. (H) Schematic drawing of the AFM experiments. Cells coexpressing RFP-Zip and GFP-Rho1 (I) or GFP-Zip and RFP-Rok[K116A] (I′) were imaged live over an average time frame of ~8 min. Stills of the movies are shown. (I) The nudging cantilever induced a rapid accumulation of Zip, but not Rho1, at the sites of deformation. (I′) Zip accumulation in response to the cantilever-imposed force preceded that of Rok. (J) The delay time of Zip mechanosensory response. Note that cells responded rapidly (< 100 s) to the mechanical force imposed by the cantilever.

(K–L′′) The mechanosensory accumulation of MyoII is dependent on its motor domain and the C-terminal BTF assembly domain. RFP-Zip[Δmotor] or RFP-Zip[ΔC] was expressed in the receiving S2R+ cells treated with Zip dsRNA. Note the absence of any mechanosensory accumulation of either Zip mutant (K and L).

(M–N′′) A positive feedback loop between Rok and MyoII. RFP-Zip or Venus-Rok[K116A] was expressed in the receiving S2R+ cells treated with Rok or Zip dsRNA. The invasive F-actin foci were marked with phalloidin staining (green in M′ and M′′; red in N′ and N′′). Note the absence of Zip or Rok accumulation in Rok (M–M′′) or Zip (N–N′′) knockdown cells.
Bars, 5 μm.

See also Movies S1 and S2.

S5B). Despite the absence of endogenous Duf or Rst in S2R+ cells, coexpressing MyoII (or Rok) with Eff-1 in the receiving cells resulted in the accumulation of MyoII (87.3% of the cases, 48/55) or Rok (81.4% of the cases, 35/43) at the fusogenic synapses (Figures 4F and 4G). In contrast, Rho1 rarely accumulated in receiving cells coexpressing Rho1 and Eff-1 (7.9% of the cases, 3/38) (Figure 4H). Taken together, results from both *Drosophila* embryos and S2R+ cells support a Rho1-independent recruitment of MyoII at the site of intercellular invasion in cell-cell fusion.

MyoII Functions as a Mechanosensor Independently of Rho and Rok

To directly test whether MyoII can respond to mechanical stimuli independently of Rho1 and Rok, we used two complementary biophysical methods, micropipette aspiration (MPA) and atomic

force microscopy (AFM). In the MPA assay, a pulling force is applied to the cell cortex via a micropipette (inner diameter, 5 μm), whereas a pushing force is applied to the cell cortex by a cantilever (100 nm width) in the AFM experiments, closely mimicking the mechanical force applied by PLS invasion in cell-cell fusion both in the direction of the force and the length scale of cortical deformation. Aspirating S2 cells expressing fluorescently tagged MyoII heavy chain (RFP-Zip) led to a rapid RFP-Zip accumulation (reaching the peak level in less than 100 s) at the tip of the cell within the micropipette (Figures 5B and 5G). In contrast, no fluorescent protein accumulation was observed in cells expressing mCherry, Rok-RFP, or Rho1-GFP within the time frame of these experiments (~10 min) (Figures 5A, 5C, 5D, and 5G). Similar mechanosensory response of MyoII was observed with AFM. Specifically, applying a mechanical

force to S2R+ cells plated on concanavalin-A-coated slides by nudging the cantilever against the cell periphery induced a rapid accumulation of RFP-Zip to the sites of deformation within tens of seconds (Figures 5H–5J; Movie S1). In contrast, Rho1 showed no accumulation in response to the pushing force (Figure 5I; Movie S1), and Rok showed a delayed accumulation compared to Zip (Figure 5I'; Movie S2). Thus, MyoII exhibits a rapid mechanosensory response, and this initial mechanosensitive accumulation occurs independent of Rho1-Rok accumulation. Moreover, MyoII accumulation does not require calcium influx, as it was unaffected by adding the calcium chelator EGTA in the medium (Figures 5E and 5G). Taken together, these results suggest that the rapid accumulation of MyoII likely results from its intrinsic ability to sense the cortical stress independent of Rho-Rok accumulation or calcium influx-mediated chemical signaling.

To investigate how MyoII may sense the cortical stress in cell-cell fusion, we characterized two Zip mutants for their localization to the fusogenic synapse in S2R+ cells. One is a headless mutant (Zip$^{\Delta motor}$), in which the motor domain was deleted, and the other is a C-terminal truncation mutant (Zip$^{\Delta C}$), which carries a deletion in the domain mediating MyoII bipolar thick filament (BTF) assembly (Uehara et al., 2010). The headless Zip$^{\Delta motor}$ mutant did not enrich at the fusogenic synapse (Figure 5K) and also failed to accumulate in the MPA assay (Figures 5F and 5G). These results suggest that mechanosensory response of MyoII is dependent on its ability to bind the actin filaments. In addition, Zip$^{\Delta C}$ also failed to enrich at the fusogenic synapse (Figure 5L). Thus, the mechanosensory function of MyoII requires both actin binding and BTF assembly.

A Positive Feedback Loop between MyoII and Rok

Although MyoII exhibited a more rapid initial mechanosensitive accumulation than Rok, they both showed steady-state enrichment in the absence of Duf and Rho signaling at the fusogenic synapse in *Drosophila* embryos and S2R+ cells. Therefore, we tested whether the steady-state enrichment of MyoII and Rok depends on each other. Knocking down Rok in the Eff-1-expressing receiving cells resulted in a failure of MyoII steady-state accumulation to the fusogenic synapse (Figure 5M), suggesting that Rok activity is required to maintain MyoII accumulation. On the other hand, knocking down MyoII in the receiving cells also abolished Rok accumulation (Figure 5N), indicating that MyoII, which was recruited earlier than Rok by mechanical force, forms a positive feedback loop with Rok to promote Rok accumulation.

MyoII Accumulation Generates Cortical Resistance to PLS Invasion

What is the cellular function of MyoII accumulation in cell-cell fusion? Given MyoII's role as a force generator, we reasoned that MyoII accumulation in founder cells may increase cortical tension/stiffness in these cells in response to the invasive force generated by the PLSs from FCMs. This model predicts that decreased MyoII activity in founder cells may enhance the penetration of PLSs emanating from FCMs due to lessened cortical resistance in the founder cells. Indeed, confocal and electron microscopy revealed wider and/or deeper invasive protrusions from FCMs into founder cells in embryos with reduced MyoII ac-
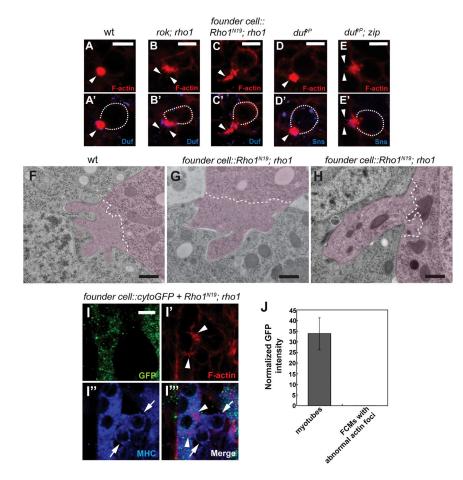
tivity (Figures 6A–6H). Specifically, while wild-type F-actin foci have a round and dense morphology with an average depth of invasion of 1.4 ± 0.3 μm (n = 30) (Figure 6A) and similar F-actin foci were observed in *duf^{rp}* mutant embryos (Figure 6D), the F-actin-enriched structures between unfused FCMs and miniature myotubes in *rok; rho1, founder cell:: Rho1^{N19}; rho1*, and *duf^{rp}; zip* mutant embryos were irregularly shaped and exhibited clearly discernable, abnormally long protrusions, with an average invasion depth of 2.5 ± 0.9 μm (n = 26), 3.5 ± 1.2 μm (n = 31), and 2.3 ± 0.8 μm (n = 31), respectively (Figures 6B, 6C, and 6E). Electron microscopy analysis revealed that wild-type FCMs projected several finger-like protrusions containing densely packed actin filaments (Figure 6F) (Sens et al., 2010). However, in *founder cell:: Rho1^{N19}; rho1* embryos, abnormally wide and/or deep invasive protrusions were observed at the tips of FCMs (Figures 6G and 6H), consistent with the PLS morphology revealed by confocal microscopy. Moreover, ribosomes and intracellular organelles were frequently observed within these abnormal protrusions (Figures 6G and 6H), indicating that the actin filaments were loosely packed. The deeper protrusions propelled by loosely packed actin filaments in these mutant embryos suggest that founder cells with decreased MyoII activity have a less elastic, softer cell cortex at the fusogenic synapse.

MyoII Activity Promotes Fusion Pore Formation

We have shown previously that actin-propelled invasive membrane protrusions are required for fusion pore formation (Duan et al., 2012; Jin et al., 2011; Sens et al., 2010; Shilagardi et al., 2013). To test whether the abnormally deep protrusions in embryos with reduced MyoII activity could promote fusion pore formation, we performed a GFP diffusion assay. This assay is based on the assumption that founder-cell-expressed cytoplasmic GFP should diffuse into the apposing FCMs upon fusion pore formation. In wild-type embryos, the originally teardrop-shaped FCM rapidly integrates into a founder cell/myotube upon fusion pore formation, making it difficult to visualize GFP diffusion from a founder cell into a rapidly integrating FCM. However, in fusion-defective mutants, unfused FCMs remain adherent to founder cells (or miniature myotubes, if fusion is only partially blocked), which should allow the visualization of GFP diffusion into FCMs if small fusion pores have opened (but failed to expand) between founder cells and the nonintegrating FCMs. Therefore, we expressed cytoplasmic GFP in founder cells of *founder cell:: Rho1^{N19}; rho1* embryos. As shown in Figures 6I and 6J, the GFP signal was tightly retained in founder cells/miniature myotubes of these embryos without diffusing into the adherent, unfused FCMs, indicating the absence of small fusion pores between founder cells/miniature myotubes and the fusion-defective FCMs. These findings suggest that the cortical resistance conferred by MyoII activation in founder cells is required for fusion pore formation.

Cortical Tension in the Receiving Fusion Partner Promotes Cell-Cell Fusion

Another prediction of the aforementioned model is that the fusion defect caused by knocking down MyoII in the receiving cells may be rescued by artificially increasing cortical tension in these cells by other means. We tested this prediction by overexpressing Fimbrin (Fim), an actin crosslinker in the receiving cells. To

Figure 6. MyoII Activity Increases Cortical Resistance Required for Fusion Pore Formation

(A–H) Deeper PLS invasion in embryos with reduced MyoII activity. (A–E′) Confocal images of F-actin foci labeled by phalloidin staining in wild-type (WT) (A and A′), *rok; rho1* (B and B′), *founder cell::Rho1^N19; rho1* (C and C′), *duf^fP* (D and D′), and *duf^fP; zip* (E and E′) embryos. Muscle cell adhesion sites labeled with α-Duf (blue) and FCMs are outlined by dashed lines. Note the roundish morphology of the F-actin focus in WT (A) and *duf^fP* (D) but the wider (B) and deeper (B, C, and E) protrusions in mutant embryos. Arrowheads indicate the tips of invasive protrusions. (F–H) Electron micrographs of the invasive PLSs in WT (F) and *founder cell::Rho1^N19; rho1* (G and H) embryos. FCMs invading founder cells are pseudocolored in pink. The F-actin-enriched areas are demarcated by dashed lines, based on the relatively low amount of ribosomes and/or intracellular organelles in these areas compared with the rest of the cell body. Note the wider (G) and deeper (G and H) protrusions, as well as the increased amount of ribosomes (G and H) and intracellular organelles (H) within the protrusions.

(I–I‴) Fusion pores fail to form between muscle cells with reduced MyoII activity. Cytoplasmic GFP was coexpressed with Rho1^N19 in founder cells of *rho1* mutant embryos stained with α-GFP (green), phalloidin (red), and α-muscle MHC (blue). Note that GFP in miniature myotubes (green in I and I‴) did not diffuse into the attached FCMs (arrows in I″ and I‴), which invaded into the myotube with deep protrusions (arrowheads in I′ and I‴).

(J) The intensity of GFP signals in myotubes versus the attached, mononucleate FCMs was quantified (n = 22 myotube-FCM pairs). Error bar indicates SEM.

Bars: (A–E and I) 5 μm; (F–H) 500 nm.

measure the cortical tension/stiffness of these cells, we again applied two complementary methods, MPA and AFM, which apply pulling and pushing forces to cells, respectively. For the ease of measurements and calculations, the round-shaped S2 cells were used as receiving cells (expressing Eff-1), which could fuse with the attacking S2R+ cells (coexpressing Sns and Eff-1) to form heterokaryotic syncytia (Figure S5C). Using AFM to measure cortical stiffness, we found that Fim overexpression not only increased the cortical stiffness of wild-type S2 cells but also restored that of MyoII-knockdown cells to wild-type levels (Figures 7A and 7B). Similarly, an increase in cortical tension caused by Fim overexpression in MyoII-knockdown cells was observed using the MPA assay (Figures S5H and S5H′). It is important to note that, although Fim overexpression did not affect membrane protrusions (Figures S5I–S5L) or cell-cell fusion in normal cells (Figure 7G; Figure S5G), it significantly rescued the fusion defects caused by MyoII knockdown (Figures 7C–7G; Figures S5C–S5G). Furthermore, Fim overexpression in the founder cells of *founder cell:: Rho1^N19; rho1* embryos significantly rescued the fusion defects in these embryos (Figures 7H–7K; Table S1). Taken together, these results support a function for MyoII in conferring cortical stiffness/tension in the receiving cells and suggest that cortical stiffness/tension in the receiving cells promotes plasma membrane fusion.

DISCUSSION

In this study, we demonstrate a critical function of MyoII-mediated cortical tension in cell-cell fusion. We show that MyoII functions as a mechanosensor in the receiving cells and accumulates at the fusogenic synapse in response to the invasive force from the attacking cells. The accumulated MyoII, in turn, increases cortical stiffness/tension in the receiving cells to promote cell-cell fusion.

MyoII Functions as a Mechanosensor in Cell-Cell Fusion

Unlike most in vivo mechanosensory systems, in which the sources and directions of the mechanical forces are difficult to pinpoint, we have uncovered a simple mechanosensory system composed of a clearly defined local force from an attacking cell and a corresponding mechanosensory response in the receiving cell during cell-cell fusion. This system makes it possible to uncouple the chemical signaling mediated by cell adhesion molecules and the mechanosensory response mediated by MyoII and to address the question of what directs the initial accumulation of MyoII to the fusogenic synapse. We found that, in both *Drosophila* embryos and cultured cells, MyoII can be recruited to, and activated at, the cortical region under the mechanical stress imposed by PLS invasion, independent of Rho1 signaling
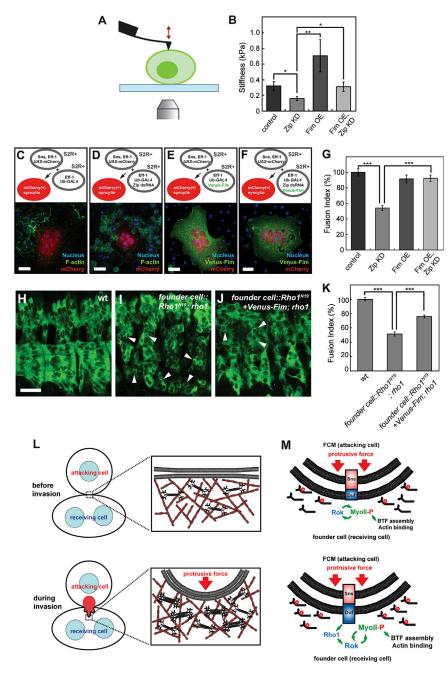
Figure 7. Artificially Increasing Cortical Tension in Receiving Cells with Decreased MyoII Activity Rescues the Fusion Defect and Models Describing the Mechanosensitive Accumulation of MyoII and the Function of Chemical Signaling in Cell-Cell Fusion

(A and B) AFM analysis of cortical stiffness. (A) Schematic drawing of the AFM experiments. (B) Measurement of cortical stiffness of S2 cells expressing Zip dsRNA and/or Fimbrin (Fim). KD, knockdown; OE, overexpression. *p < 0.05 and **p < 0.01. Error bars indicate SEM.

(C–G) Fim overexpression rescued the fusion defect caused by Zip KD in the receiving cells. (C–F) Schematic representations and confocal images of cell-cell fusion in S2R+ cells. Attacking cells expressing Sns, Eff-1, and *UAS-mCherry* were mixed with receiving cells expressing Eff-1, *ubiquitin (Ub)-GAL4*, and Zip dsRNA (D and F) or Venus-Fim (E and F). Cells were stained with DAPI (nuclei; blue) and phalloidin (F-actin; green) (C and D). (G) Statistical analysis of cell fusion. The fusion index was calculated as percentage of the average nuclei number in mCherry-positive syncytia (n > 65) in (D), (E), or (F) versus that in (C). Fusion between attacking and receiving cells was indicated by mCherry expression in the multinucleate syncytia (red). Bars, 5 μm.

(H–K) Fim overexpression in founder cells significantly rescues the fusion defect in embryos with decreased MyoII activity. Stage 15 *founder cell::Rho1N19; rho1* embryos were labeled as in Figure 1. Arrowheads indicate unfused FCMs. The fusion index was quantified in (K). Bar, 20 μm. Error bars indicate SEM. ***p < 10^{-4}.

(L) Cortical deformation by PLS invasion induces MyoII accumulation. Prior to PLS invasion, the cortical actin network is under less tension and only a few MyoII BTF are present. During PLS invasion, the protrusive force from the attacking cell deforms the cortical actin network in the receiving cell. Actin network deformation, in turn, applies load to the bound MyoII BTFs and cause MyoII stalling on the strained actin filaments. More BTFs then cooperatively bind to these strained actin filament, ultimately leading to the accumulation of MyoII in response to the mechanical stress.

(M) Rho1 signaling mediated by cell adhesion molecules enhances MyoII activation at the fusogenic synapse. In the absence of Duf-mediated Rho1 accumulation/activation at the fusogenic synapse, MyoII is activated by the basal level of Rok in the cytoplasm and forms a feedback loop with Rok. In the presence of Duf-mediated Rho1 signaling, more freely diffusible MyoII are phosphorylated and activated, providing additional BTFs for binding to strained actin network.

See also Figure S5.

induced by cell adhesion molecules. Moreover, MyoII exhibits a rapid mechanosensitive accumulation in response to externally applied force in cultured cells, preceding that of Rok and Rho1. These findings strongly support a role of MyoII as a direct sensor for mechanical stress independent of chemical signaling mediated by cell adhesion molecules and Rho1.

How does MyoII sense mechanical stress? Previous in vitro studies of several myosins, including MyoII, have demonstrated that mechanical resistance keeps myosin in the ADP-bound state, locking the myosin motor on the actin filament (Kee and Robinson, 2008; Kovács et al., 2007; Laakso et al., 2008; Purcell et al., 2005). When stalled at the isomeric binding state, the myosin motors can trigger cooperative binding of additional freely diffusing myosin to the actin filament (Luo et al., 2012). In this study, we find that the mechanosensory function of MyoII is dependent on F-actin binding, since the headless mutant does not show mechanosensitive accumulation either in the cell-fusion culture system or in the MPA assay. Similar

dependence of F-actin binding has been shown for MPA-induced MyoII mechanosensitive accumulation in *Dictyostelium* (Luo et al., 2012; Ren et al., 2009). We propose that, during cell-cell fusion, the mechanical force imposed on the receiving cell deforms and strains the cortical actin network, which, in turn, applies load on the actin-bound bipolar thick filaments of MyoII (activated by the basal level of cytoplasmic Rho1 and Rok), leading to the stalling, cooperative binding, and, ultimately, mechanosensitive accumulation of MyoII at the mechanically deformed fusogenic synapse (Figure 7L). Thus, by sensing the strain in the actin network, MyoII is repositioned to specific cellular locations in response to mechanical stimuli. Based on our findings from this simple mechanosensory system, we propose that mechanical tension plays a general role in directing MyoII accumulation to specific cellular locations in vivo.

Our study has also revealed an intimate coordination between the mechanosensory response of MyoII and the chemical signaling mediated by cell adhesion molecules. We show that the initial accumulation of MyoII is stabilized by a positive feedback loop between Rok and MyoII. The coaccumulation of MyoII and Rok at the fusogenic synapse in the absence of Rho1 signaling appears to be sufficient to induce a high percentage of cell-cell fusion in cultured cells and to partially rescue the myoblast fusion defect in *duf,rst* mutant embryos. However, in wild-type embryos, more efficient cell-cell fusion (~11 min per fusion event versus ~30 min in cultured cells) (Richardson et al., 2007; Shilagardi et al., 2013) does incorporate the input from Rho1 signaling mediated by cell adhesion molecules. The Rho1 accumulation and activation at the fusogenic synapse in *Drosophila* embryos provides spatiotemporal coupling of Rho1 signaling to the fusion event. Such spatiotemporal coupling helps generate more activated, freely diffusible MyoII monomers, which are then available to participate in BTF assembly, thereby amplifying the MyoII mechanosensory response at the fusogenic synapse (Figure 7M).

Mechanical Tension Drives Cell Membrane Fusion

A critical barrier for fusing all biological membranes is to bring the two membranes destined to fuse into close proximity. In cell-cell fusion, the initial plasma membrane apposition is mediated by cell adhesion molecules. However, cell adhesion is not sufficient to induce cell-cell fusion, as demonstrated by studies in cultured cells (Shilagardi et al., 2013). Consistent with this observation, recent crystallographic studies have shown that Duf and Sns form a rigid L-shaped structure that props the plasma membranes ~45 nm apart, a distance too large for membrane fusion to occur (Özkan et al., 2014). To overcome this distance, cells utilize an actin-based invasive mechanism, in which one cell (the attacking cell) extends finger-like protrusions into its fusion partner (the receiving cell), to push the plasma membranes into closer proximity for fusogen engagement and fusion pore formation (Sens et al., 2010; Shilagardi et al., 2013). Our current study demonstrates that the protrusive force generated by the Arp2/3-based actin polymerization from the attacking cell is counteracted by increased cortical tension/stiffness generated by the actomyosin network in the receiving cells. This counteractive force is critical for cell-cell fusion, since reducing cortical tension/stiffness in the receiving cell inhibits fusion, despite the presence of long and deep protrusions from the attacking cell.

The MyoII-mediated cortical tension in the receiving cell may serve multiple roles in cell-cell fusion. First, it provides resistance in the receiving cell so that its plasma membrane would not be pushed away by the invasive protrusions from the attacking cell, in effect promoting plasma membrane proximity. Second, the cortical tension in the receiving cell may also provide a positive feedback to the actin network within the invasive protrusions from the attacking cell. In support of this view, the "softer" cortex of the MyoII-knockdown receiving cell is invaded by "weaker" protrusions propelled by loosely packed actin filaments, whereas receiving cells with normal cortical stiffness are invaded by stiffer protrusions propelled by densely packed actin filaments. In this regard, it has been shown that mechanical stresses applied to the actin networks induce network stiffening, through either the engagement of more actin crosslinkers or an increase in Arp2/3-based actin polymerization (Chaudhuri et al., 2007; Gardel et al., 2004; Risca et al., 2012; Xu et al., 2000). Thus, pushing against a stiff cortex of the receiving cell induces stiffness of the invasive protrusions from the attacking cell, which, in turn, triggers stronger mechanosensory response and cortical tension in the receiving cell. We propose that this positive feedback between a pair of mechanical forces—the protrusive force from the attacking cell and the resisting force from the receiving cell—put the fusogenic synapse under high mechanical tension, which helps to overcome the energy barriers to bring the apposing cell membranes into close proximity for fusion. Whether and how the cortical tension generated by the asymmetric actin polymerization and actomyosin contraction at the fusogenic synapse affects the in-plane plasma membrane tension require future investigation. Nevertheless, our analyses of both *Drosophila* myoblast fusion and the reconstituted cell-fusion culture system suggest that the interplay of mechanical forces between two fusion partners is a general mechanism driving cell membrane fusion.

EXPERIMENTAL PROCEDURES

Fly Genetics
See the Supplemental Experimental Procedures for fly stocks used in this study and fly crosses for gene expression and rescue experiments.

Immunohistochemistry
Fly embryos were fixed and stained as described elsewhere (Kim et al., 2007; Sens et al., 2010). See the Supplemental Experimental Procedures for primary and secondary antibodies used in this study. Fluorescent images were obtained on an LSM 700 Meta confocal microscope (Zeiss), acquired with LSM Image Browser software (Zeiss) and Zen software (Zeiss), and processed using Adobe Photoshop CS. For quantification of fluorescent signals, the signal intensity of cellular areas of interest and control areas was measured using the ImageJ program (http://imagej.nih.gov/ij/) and normalized by subtracting the background intensity.

Molecular Biology
Full-length and partial cDNAs of *rho1*, *zip*, and *fim* were amplified by PCR from EST clones obtained from the *Drosophila* Genome Resource Center (DGRC). All expression constructs were generated using pAc or pUAST vectors with GFP, Venus, RFP, or hemagglutinin (HA) tags. See Supplemental Experimental Procedures for double-stranded RNA (dsRNA) synthesis and purification.

Electron Microscopy
The high-pressure freezing and freeze substitution (HPF/FS) method was used to fix fly embryos as described elsewhere (Sens et al., 2010; Zhang and Chen, 2008). See the Supplemental Experimental Procedures for details.

Cell Culture, Transfection, RNAi, and Immunocytochemistry

S2R+ cells and S2 cells were cultured, fixed, and stained as described elsewhere (Shilagardi et al., 2013). See the Supplemental Experimental Procedures for details.

Rho1 Pull-Down Assay

GST-Rhotekin-RBD protein conjugated to agarose beads (Cytoskeleton) were used to pull down GTP-bound Rho1 in S2R+ cells. See the Supplemental Experimental Procedures for details.

Reconstitution of Cell-Cell Fusion in Cultured Cells

S2R+ cell fusion was induced as described elsewhere (Shilagardi et al., 2013). Briefly, two groups of S2R+ cells (or a group of S2R+ cells and a group of S2 cells) were transfected independently in a six-well plate. The "attacking" cells were transfected with Sns-V5, Eff-1-HA, and UAS-mCherry, and the "receiving" S2R+ (or S2 cells) were transfected with Eff-1-HA, Ub-GAL4, and other appropriate constructs. Cells were incubated for 12–16 hr, washed, and harvested by trypsinization and centrifugation. Harvested cells were washed, resuspended, mixed with the appropriate group of fusion partners at a 1:1 ratio, and seeded onto coverslips. The mixed cell populations were fixed and stained at 48 hr after mixing. Intergroup cell fusion was monitored by mCherry expression.

Micropipette Aspiration Assay

The MPA assay system was set up as described elsewhere (Effler et al., 2006; Kee and Robinson, 2013; Ren et al., 2009). The suction pressure was applied to the cell cortex with a polished glass pipette ($\sim$2.5 μm in radius, R_p). For cortical tension measurements, the aspiration pressure was increased to the equilibrium pressure (ΔP) at which the length of the cell inside the pipette (L_p) was equal to R_p. The effective cortical tension (T_{eff}) was determined by the Young-Laplace equation: $\Delta p = 2T_{eff}(1/R_p - 1/R_c)$, where R_c is the radius of the cell and ΔP is the equilibrium pressure when $L_p = R_p$ (Derganc et al., 2000; Octtaviani et al., 2006). For mechanosensory response studies, each cell was aspirated for at least 10 min to ensure enough time for mechanosensitive protein accumulation. Epifluorescence images were taken to monitor the protein localization during MPA. Cells were imaged using an Olympus 1X81 microscope with a 40× (NA, 1.3) objective with 1.6× Optovar. All images were acquired using the MetaMorph Software (Molecular Devices) and processed using ImageJ program. Background-subtracted protein pixel intensities at the tip of the cell body within the pipette and at the opposite pole of the cell body were measured, and the ratio was calculated and used for statistical analysis. Statistical analysis was performed using KaleidaGraph (Synergy Software). An ANOVA with Fisher's least significant difference post hoc test was applied. Only p values less than 0.05 were considered significant.

Atomic Force Microscopy

Experiments were conducted at room temperature using a BioScope Catalyst Atomic Force Microscope (Bruker AXS) with a sample stage mounted atop an inverted optical microscope (Zeiss Axio Observer Z1, Carl Zeiss). Data acquisition and atomic force microscopy (AFM) control were performed using the NanoScope software (Bruker). MLCT-C cantilevers (Bruker) with a nominal spring constant of 10 pN/nm were used in all experiments. The actual spring constant of each cantilever was determined by thermal calibration in air. Prior to the cortical stiffness measurement, S2 cells were plated on a glass coverslip coated with high-molecular-weight poly-L-lysine (Sigma), which immobilized cells without spreading. Cells were indented at the rate of 100 nm/s to avoid contribution of viscosity on elasticity measurements. The Young's Modulus of elasticity was calculated by fitting the cantilever deflection versus piezo extension curves to the modified Hertz model as described elsewhere (Rosenbluth et al., 2006), using a custom-written algorithm in MATLAB (Mathworks). Student's t test was used to determine whether the differences in average elasticities were statistically significant.

For lateral indentation experiments, S2R+ cells were plated on glass coverslips coated with concanavalin A (Sigma) and transfected with fluorescently tagged Zip, Rok^{K116A}, or Rho1 using Effectene (QIAGEN). Lateral indentation experiments were conducted 3 days after transfection. To determine the effect of a localized mechanical force on Zip, Rok^{K116A}, or Rho1 localization, the cantilever (100-nm width) (MLCT or DNP with a pyramidal tip, Bruker) was first brought into full contact, at around 50 nN setpoint force, with the glass surface on a cell-free area within 10 μm from a target cell. Next, the cell was laterally translated into the stationary cantilever using the piezoelectric XY stage and the NanoScope software (Bruker). The cantilever tip indented the edge of the cell by 2–5 μm. Cells were simultaneously imaged by epifluorescence with a plan-apochromat 100×/1.46 NA oil immersion objective (Zeiss). Time-lapse images were taken at 2-s intervals using the Micro-Manager software (http://micro-manager.org/wiki/Micro-Manager).

SUPPLEMENTAL INFORMATION

Supplemental Information includes Supplemental Experimental Procedures, five figures, one table, and two movies and can be found with this article online at http://dx.doi.org/10.1016/j.devcel.2015.01.005.

REFERENCES

Abmayr, S.M., and Pavlath, G.K. (2012). Myoblast fusion: lessons from flies and mice. Development *139*, 641–656.

Abmayr, S.M., Zhuang, S., and Geisbrecht, E.R. (2008). Myoblast fusion in Drosophila. Methods Mol. Biol. *475*, 75–97.

Aguilar, P.S., Baylies, M.K., Fleissner, A., Helming, L., Inoue, N., Podbilewicz, B., Wang, H., and Wong, M. (2013). Genetic basis of cell-cell fusion mechanisms. Trends Genet. *29*, 427–437.

Aguilar-Cuenca, R., Juanes-García, A., and Vicente-Manzanares, M. (2014). Myosin II in mechanotransduction: master and commander of cell migration, morphogenesis, and cancer. Cell. Mol. Life Sci. *71*, 479–492.

Amano, M., Ito, M., Kimura, K., Fukata, Y., Chihara, K., Nakano, T., Matsuura, Y., and Kaibuchi, K. (1996). Phosphorylation and activation of myosin by Rho-associated kinase (Rho-kinase). J. Biol. Chem. *271*, 20246–20249.

Artero, R.D., Castanon, I., and Baylies, M.K. (2001). The immunoglobulin-like protein Hibris functions as a dose-dependent regulator of myoblast fusion and is differentially controlled by Ras and Notch signaling. Development *128*, 4251–4264.

Bour, B.A., Chakravarti, M., West, J.M., and Abmayr, S.M. (2000). Drosophila SNS, a member of the immunoglobulin superfamily that is essential for myoblast fusion. Genes Dev. *14*, 1498–1511.

Bulchand, S., Menon, S.D., George, S.E., and Chia, W. (2010). The intracellular domain of Dumbfounded affects myoblast fusion efficiency and interacts with Rolling pebbles and Loner. PLoS ONE *5*, e9374.

Chaudhuri, O., Parekh, S.H., and Fletcher, D.A. (2007). Reversible stress softening of actin networks. Nature *445*, 295–298.

Chen, E.H. (2011). Invasive podosomes and myoblast fusion. Curr. Top. Membr. *68*, 235–258.

Chen, E.H., and Olson, E.N. (2004). Towards a molecular pathway for myoblast fusion in Drosophila. Trends Cell Biol. *14*, 452–460.

Chen, E.H., and Olson, E.N. (2005). Unveiling the mechanisms of cell-cell fusion. Science *308*, 369–373.

Derganc, J., Bozic, B., Svetina, S., and Zeks, B. (2000). Stability analysis of micropipette aspiration of neutrophils. Biophys. J. 79, 153–162.

Discher, D.E., Mooney, D.J., and Zandstra, P.W. (2009). Growth factors, matrices, and forces combine and control stem cells. Science 324, 1673–1677.

Doherty, G.J., and McMahon, H.T. (2009). Mechanisms of endocytosis. Annu. Rev. Biochem. 78, 857–902.

Dottermusch-Heidel, C., Groth, V., Beck, L., and Önel, S.F. (2012). The Arf-GEF Schizo/Loner regulates N-cadherin to induce fusion competence of Drosophila myoblasts. Dev. Biol. 368, 18–27.

Duan, R., Jin, P., Luo, F., Zhang, G., Anderson, N., and Chen, E.H. (2012). Group I PAKs function downstream of Rac to promote podosome invasion during myoblast fusion in vivo. J. Cell Biol. 199, 169–185.

Dworak, H.A., Charles, M.A., Pellerano, L.B., and Sink, H. (2001). Characterization of Drosophila hibris, a gene related to human nephrin. Development 128, 4265–4276.

Effler, J.C., Kee, Y.S., Berk, J.M., Tran, M.N., Iglesias, P.A., and Robinson, D.N. (2006). Mitosis-specific mechanosensing and contractile-protein redistribution control cell shape. Curr. Biol. 16, 1962–1967.

Farge, E. (2011). Mechanotransduction in development. Curr. Top. Dev. Biol. 95, 243–265.

Fernandez-Gonzalez, R., Simoes, Sde.M., Röper, J.C., Eaton, S., and Zallen, J.A. (2009). Myosin II dynamics are regulated by tension in intercalating cells. Dev. Cell 17, 736–743.

Gardel, M.L., Shin, J.H., MacKintosh, F.C., Mahadevan, L., Matsudaira, P., and Weitz, D.A. (2004). Elastic behavior of cross-linked and bundled actin networks. Science 304, 1301–1305.

Gauthier, N.C., Masters, T.A., and Sheetz, M.P. (2012). Mechanical feedback between membrane tension and dynamics. Trends Cell Biol. 22, 527–535.

Geisbrecht, E.R., Haralalka, S., Swanson, S.K., Florens, L., Washburn, M.P., and Abmayr, S.M. (2008). Drosophila ELMO/CED-12 interacts with Myoblast city to direct myoblast fusion and ommatidial organization. Dev. Biol. 314, 137–149.

Guillot, C., and Lecuit, T. (2013). Mechanics of epithelial tissue homeostasis and morphogenesis. Science 340, 1185–1189.

Haralalka, S., Shelton, C., Cartwright, H.N., Katzfey, E., Janzen, E., and Abmayr, S.M. (2011). Asymmetric Mbc, active Rac1 and F-actin foci in the fusion-competent myoblasts during myoblast fusion in Drosophila. Development 138, 1551–1562.

Jahn, R., and Südhof, T.C. (1999). Membrane fusion and exocytosis. Annu. Rev. Biochem. 68, 863–911.

Jahn, R., and Fasshauer, D. (2012). Molecular machines governing exocytosis of synaptic vesicles. Nature 490, 201–207.

Jin, P., Duan, R., Luo, F., Zhang, G., Hong, S.N., and Chen, E.H. (2011). Competition between Blown fuse and WASP for WIP binding regulates the dynamics of WASP-dependent actin polymerization in vivo. Dev. Cell 20, 623–638.

Kee, Y.S., and Robinson, D.N. (2008). Motor proteins: myosin mechanosensors. Curr. Biol. 18, R860–R862.

Kee, Y.S., and Robinson, D.N. (2013). Micropipette aspiration for studying cellular mechanosensory responses and mechanics. Methods Mol. Biol. 983, 367–382.

Kielian, M., and Rey, F.A. (2006). Virus membrane-fusion proteins: more than one way to make a hairpin. Nat. Rev. Microbiol. 4, 67–76.

Kim, S., Shilagardi, K., Zhang, S., Hong, S.N., Sens, K.L., Bo, J., Gonzalez, G.A., and Chen, E.H. (2007). A critical function for the actin cytoskeleton in targeted exocytosis of prefusion vesicles during myoblast fusion. Dev. Cell 12, 571–586.

Kovács, M., Thirumurugan, K., Knight, P.J., and Sellers, J.R. (2007). Load-dependent mechanism of nonmuscle myosin 2. Proc. Natl. Acad. Sci. USA 104, 9994–9999.

Laakso, J.M., Lewis, J.H., Shuman, H., and Ostap, E.M. (2008). Myosin I can act as a molecular force sensor. Science 321, 133–136.

Lecuit, T., Lenne, P.F., and Munro, E. (2011). Force generation, transmission, and integration during cell and tissue morphogenesis. Annu. Rev. Cell Dev. Biol. 27, 157–184.

Luo, T., Mohan, K., Srivastava, V., Ren, Y., Iglesias, P.A., and Robinson, D.N. (2012). Understanding the cooperative interaction between myosin II and actin cross-linkers mediated by actin filaments during mechanosensation. Biophys. J. 102, 238–247.

Luo, T., Mohan, K., Iglesias, P.A., and Robinson, D.N. (2013). Molecular mechanisms of cellular mechanosensing. Nat. Mater. 12, 1064–1071.

Mammoto, T., Mammoto, A., and Ingber, D.E. (2013). Mechanobiology and developmental control. Annu. Rev. Cell Dev. Biol. 29, 27–61.

Martens, S., and McMahon, H.T. (2008). Mechanisms of membrane fusion: disparate players and common principles. Nat. Rev. Mol. Cell Biol. 9, 543–556.

Melikyan, G.B. (2008). Common principles and intermediates of viral protein-mediated fusion: the HIV-1 paradigm. Retrovirology 5, 111.

Octtaviani, E., Effler, J.C., and Robinson, D.N. (2006). Enlazin, a natural fusion of two classes of canonical cytoskeletal proteins, contributes to cytokinesis dynamics. Mol. Biol. Cell 17, 5275–5286.

Özkan, E., Chia, P.H., Wang, R.R., Goriatcheva, N., Borek, D., Otwinowski, Z., Walz, T., Shen, K., and Garcia, K.C. (2014). Extracellular architecture of the SYG-1/SYG-2 adhesion complex instructs synaptogenesis. Cell 156, 482–494.

Prokop, A., Martín-Bermudo, M.D., Bate, M., and Brown, N.H. (1998). Absence of PS integrins or laminin A affects extracellular adhesion, but not intracellular assembly, of hemiadherens and neuromuscular junctions in Drosophila embryos. Dev. Biol. 196, 58–76.

Purcell, T.J., Sweeney, H.L., and Spudich, J.A. (2005). A force-dependent state controls the coordination of processive myosin V. Proc. Natl. Acad. Sci. USA 102, 13873–13878.

Ren, Y., Effler, J.C., Norstrom, M., Luo, T., Firtel, R.A., Iglesias, P.A., Rock, R.S., and Robinson, D.N. (2009). Mechanosensing through cooperative interactions between myosin II and the actin crosslinker cortexillin I. Curr. Biol. 19, 1421–1428.

Richardson, B.E., Beckett, K., Nowak, S.J., and Baylies, M.K. (2007). SCAR/WAVE and Arp2/3 are crucial for cytoskeletal remodeling at the site of myoblast fusion. Development 134, 4357–4367.

Risca, V.I., Wang, E.B., Chaudhuri, O., Chia, J.J., Geissler, P.L., and Fletcher, D.A. (2012). Actin filament curvature biases branching direction. Proc. Natl. Acad. Sci. USA 109, 2913–2918.

Rochlin, K., Yu, S., Roy, S., and Baylies, M.K. (2010). Myoblast fusion: when it takes more to make one. Dev. Biol. 341, 66–83.

Rosenbluth, M.J., Lam, W.A., and Fletcher, D.A. (2006). Force microscopy of nonadherent cells: a comparison of leukemia cell deformability. Biophys. J. 90, 2994–3003.

Ruiz-Gómez, M., Coutts, N., Price, A., Taylor, M.V., and Bate, M. (2000). Drosophila dumbfounded: a myoblast attractant essential for fusion. Cell 102, 189–198.

Sapir, A., Avinoam, O., Podbilewicz, B., and Chernomordik, L.V. (2008). Viral and developmental cell fusion mechanisms: conservation and divergence. Dev. Cell 14, 11–21.

Sens, K.L., Zhang, S., Jin, P., Duan, R., Zhang, G., Luo, F., Parachini, L., and Chen, E.H. (2010). An invasive podosome-like structure promotes fusion pore formation during myoblast fusion. J. Cell Biol. 191, 1013–1027.

Shelton, C., Kocherlakota, K.S., Zhuang, S., and Abmayr, S.M. (2009). The immunoglobulin superfamily member Hbs functions redundantly with Sns in interactions between founder and fusion-competent myoblasts. Development 136, 1159–1168.

Shilagardi, K., Li, S., Luo, F., Marikar, F., Duan, R., Jin, P., Kim, J.H., Murnen, K., and Chen, E.H. (2013). Actin-propelled invasive membrane protrusions promote fusogenic protein engagement during cell-cell fusion. Science 340, 359–363.

Simões, Sde.M., Blankenship, J.T., Weitz, O., Farrell, D.L., Tamada, M., Fernandez-Gonzalez, R., and Zallen, J.A. (2010). Rho-kinase directs Bazooka/Par-3 planar polarity during Drosophila axis elongation. Dev. Cell 19, 377–388.

Strünkelnberg, M., Bonengel, B., Moda, L.M., Hertenstein, A., de Couet, H.G., Ramos, R.G., and Fischbach, K.F. (2001). rst and its paralogue kirre act redundantly during embryonic muscle development in Drosophila. Development *128*, 4229–4239.

Uehara, R., Goshima, G., Mabuchi, I., Vale, R.D., Spudich, J.A., and Griffis, E.R. (2010). Determinants of myosin II cortical localization during cytokinesis. Curr. Biol. *20*, 1080–1085.

Vogel, V., and Sheetz, M.P. (2009). Cell fate regulation by coupling mechanical cycles to biochemical signaling pathways. Curr. Opin. Cell Biol. *21*, 38–46.

Xu, J., Tseng, Y., and Wirtz, D. (2000). Strain hardening of actin filament networks. Regulation by the dynamic cross-linking protein alpha-actinin. J. Biol. Chem. *275*, 35886–35892.

Zajac, A.L., and Discher, D.E. (2008). Cell differentiation through tissue elasticity-coupled, myosin-driven remodeling. Curr. Opin. Cell Biol. *20*, 609–615.

Zhang, S., and Chen, E.H. (2008). Ultrastructural analysis of myoblast fusion in *Drosophila*. In Cell Fusion: Overviews and Methods, E.H. Chen, ed. (New Jersey: Humana Press), pp. 275–297.